Single-Dose Versus Fractionated Radioimmunotherapy: Model Comparisons for Uniform Tumor Dosimetry

Joseph A. O'Donoghue, George Sgouros, Chaitanya R. Divgi, and John L. Humm

Department of Medical Physics and Nuclear Medicine Service, Memorial Sloan-Kettering Cancer Center, New York, New York

Targeting molecules with reduced immunogenicity will enable repetitive administrations of radioimmunotherapy. In this work a mathematical model was used to compare 2 different treatment strategies: large single administrations (LSAs) and rapid fractionation (RF) of small individual administrations separated by short time intervals. **Methods:** An integrated compartmental model of treatment pharmacokinetics and tumor response was used to compare alternative treatments that delivered identical absorbed doses to red marrow. **Results:** Based on the key assumption of uniform dose distributions, the LSA approach consistently produced smaller nadir values of tumor cell survival and tumor size. The predicted duration of remission was similar for both treatment structures. These findings held for both macroscopic and microscopic tumors and were independent of tumor cell radiosensitivity, proliferation rate, rate of tumor shrinkage, and uptake characteristics of radiolabeled material in tumor. **Conclusion:** Clinical situations for which each treatment is most appropriate may be tentatively identified. An LSA using a short-range–emitting radionuclide would be most appropriate for therapy of microscopic disease, if uptake is relatively homogeneous. RF using a longer range emitter would be most appropriate for macroscopic disease, if uptake is heterogeneous and varies from one administration to another. There is a rationale for combining LSA and RF treatments in clinical situations in which slowly growing macroscopic disease and rapidly growing microscopic disease exist simultaneously.

Key Words: radioimmunotherapy; tumor response; Gompertzian growth; cure; remission; fractionation; mathematical model

J Nucl Med 2000; 41:538–547

Until recently, the immunogenicity of targeting molecules has restricted the applicability of repetitive administrations of radioimmunotherapy (RIT). However, recent advances in biotechnology have generated molecules (such as chimeric or humanized antibodies) that may enable repeat treatments without the induction of a significant immune response (*1–3*).

Received Nov. 6, 1998; revision accepted Jul. 21, 1999.

For correspondence or reprints contact: Joseph A. O'Donoghue, PhD, Department of Medical Physics, Memorial Sloan-Kettering Cancer Center, 1275 York Ave., New York, NY 10021.

It is not self-evident that multiple administrations will increase the effectiveness of RIT. Prolongation of conventional external beam radiotherapy (XRT) is associated with a reduction in therapeutic response (*4–6*), usually attributed to allowing more time for tumor cell proliferation (*7–9*). Moreover, a major radiobiologic advantage associated with fractionated XRT is the differential increase in repair of radiation damage in late-responding normal tissues compared with tumors. This is unlikely to be applicable to targeted radionuclide therapy because absorbed dose rates are usually so low that repair is effectively complete, irrespective of the treatment structure (*10,11*). However, multiple administrations may allow some degree of proliferative recovery by bone marrow, thus enabling an increase in the allowable absorbed dose (*12*). In addition, the effects of preceding therapeutic administrations on tumor architecture may enable subsequent administrations to target tumor regions inaccessible to single administrations. This would improve the uniformity of absorbed dose distributions in tumors and thereby increase the therapeutic effectiveness. Data from animal experiments suggest that a series of relatively small administrations, each separated by several days, is both intrinsically more tumoricidal and less toxic to bone marrow than a large single administration (LSA) (*13–15*).

This article describes the application of a mathematical model (*16*) of tumor response to RIT. The model is used to examine some of the factors that influence the therapeutic effects of alternative administration patterns. Two generic treatment structures are compared: an LSA and a course of rapid fractionation (RF) of small administrations. These are calculated to deliver the same total absorbed dose to red marrow. The absorbed dose rate in tumors is derived using a pharmacokinetic model. For both treatment structures, absorbed doses and dose rates in tumors are assumed to be uniform. Attention is focused on ^{131}I, as this is the most commonly used radionuclide for RIT at present, but the methodology is applicable to any therapy radionuclide. The proliferative response of tumors is described by a Gompertzian relationship and is thus size dependent. This enables

a distinction to be made between treatment of macroscopic and microscopic disease.

METHODS AND MATERIALS

Pharmacokinetic Model

The biodistribution of radiolabeled targeting molecules is described using the simple 3-compartmental model shown in Figure 1. A model similar to this has previously been validated using clinical data derived from a phase I/II clinical trial of RIT with ^{131}I-labeled murine anti-G250 antibody for renal cell cancer (*17*). In this study, only whole-body and serum activities were considered, and a tumor compartment was not included. In the current model, the tumor compartment represents a dynamic system, capable of growth or regression depending on the effects of therapy. Radiolabeled material is administered to a source compartment, from which it exchanges with the other compartments. The source compartment is assumed here to be serum and the extravascular space of rapidly accessible organs. The "rest-of-body" compartment represents a combination of normal tissue sinks that take up radiolabeled molecules and may rerelease them to serum. The process of excretion is envisaged to remove agent from the rest of the body and not directly from serum.

The kinetic behavior of this system is determined by the differential equations:

$$\frac{d}{dt}E = -t_1E + t_2T - r_1E + r_2R, \qquad \text{Eq. 1}$$

$$\frac{d}{dt}T = t_1E - t_2T, \qquad \text{Eq. 2}$$

and

$$\frac{d}{dt}R = r_1E - r_2R - e_1R, \qquad \text{Eq. 3}$$

where E, T, and R are the number of molecules in the serum, tumor, and rest-of-body compartments, and t_1, t_2, r_1, r_2, and e_1 are the respective rate parameters. The serum and rest-of-body compartments are taken to be of fixed size. It is also assumed that they are of sufficient size, with respect to the concentration of radiolabeled material, that the respective rate parameters (r_1, r_2, e_1) may be considered constants. For the tumor, the simplest scenario involves exponential (i.e., size independent) loss of radiolabeled material. In this case, the rate parameter (t_2) may also be considered constant. The rate parameter for tumor uptake (t_1), however, must incorporate some dependency on tumor size. The simplest possibility is $t_1 = \tau vol_T$, where vol_T is the tumor volume and τ is a constant. This means that uptake, in terms of number of molecules, is proportional to tumor volume. With this modification, Equations 1–3 can be reformulated in terms of concentrations as:

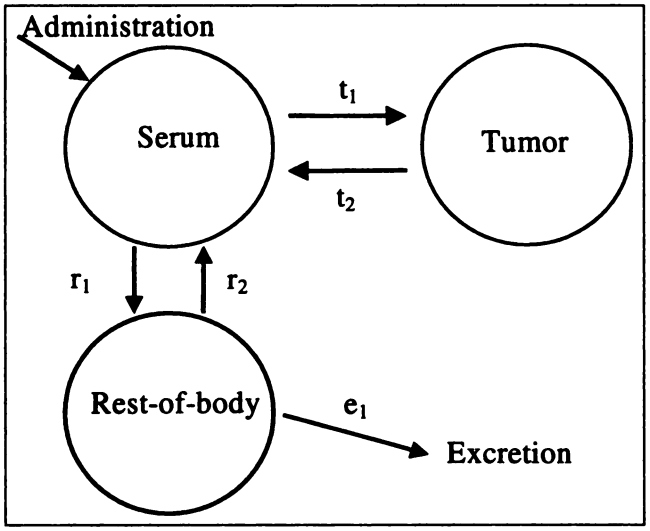

FIGURE 1. Compartmental model used to calculate pharmacokinetic behavior of system. Size of tumor compartment varies dynamically depending on effects of therapy.

$$\frac{d}{dt}[E] = -\tau vol_T[E] + t_2[T]\left(\frac{vol_T}{vol_E}\right) - r_1[E] + r_2R\left(\frac{1}{vol_E}\right), \qquad \text{Eq. 4}$$

$$\frac{d}{dt}[T] = \tau[E]vol_E - t_2[T], \qquad \text{Eq. 5}$$

and

$$\frac{d}{dt}R = r_1[E]vol_E - r_2R - e_1R, \qquad \text{Eq. 6}$$

where vol_E is the serum volume of distribution.

The time–activity profiles for the 3 compartments are generated numerically using Euler's method. The concentration or absolute quantity of activity (Z) in any compartment for time period i is derived from that for the previous time period (i − 1) by:

$$(Z)_i = I_i + ((Z)_{i-1} + \Delta(Z))\exp(-k\Delta t), \qquad \text{Eq. 7}$$

where k is the decay constant of the radionuclide (= $\ln 2/T_{1/2}$), Δt is the time increment between periods, and I_i is any direct input pulse of radiolabeled material occurring in time period i. In effect, I_i is 0 for all compartments at all times, except for the serum compartment at the specific times when activity is administered. The actual increments (ΔZ) for each of the compartments derived from Equations 4–6 are as follows:

$$\Delta[E] = \left\{-\tau vol_{T(i-1)}[E]_{i-1} + t_2[T]_{i-1}\left(\frac{vol_{T(i-1)}}{vol_E}\right) - r_1[E]_{i-1} + r_2R_{i-1}\left(\frac{1}{vol_E}\right)\right\}\Delta t, \qquad \text{Eq. 8}$$

$$\Delta[T] = \{\tau[E]_{i-1}vol_E - t_2[T]_{i-1}\}\Delta t, \qquad \text{Eq. 9}$$

and

$$\Delta R = \{r_1[E]_{i-1}vol_E - r_2R_{i-1} - e_1R_{i-1}\}\Delta t. \qquad \text{Eq. 10}$$

Equations 8–10, together with the general relationship given by Equation 7, are used to model the kinetic behavior of radiolabeled material throughout the system.

For the case where $t_1(vol_T) = \tau(vol_T)^{2/3}$, then Equations 8 and 9 must be replaced by:

$$\Delta[E] = \left\{-\tau(vol_{T(i-1)})^{2/3}[E]_{i-1} + t_2[T]_{i-1}\left(\frac{vol_{T(i-1)}}{vol_E}\right) - r_1[E]_{i-1} + r_2R_{i-1}\left(\frac{1}{vol_E}\right)\right\}\Delta t, \qquad \text{Eq. 11}$$

$$\Delta[T] = \{\tau(vol_{T(i-1)})^{-1/3}[E]_{i-1}(vol_E) - t_2[T]_{i-1}\}\Delta t. \qquad \text{Eq. 12}$$

Activity in the tumor generates an absorbed-radiation dose rate. The mean absorbed dose rate r, because of self-irradiation, is expressed by the product of the activity concentration in the tumor [A], the absorbed fraction θ, and the equilibrium dose constant Δ, i.e.:

$$r = [A]\phi\Delta. \qquad \text{Eq. 13}$$

Model of Tumor Response to Irradiation

The mathematical model describing the response of the tumor to radiation treatment has been presented in detail elsewhere (*16*) and is represented schematically in Figure 2. The main features and assumptions of this model are as follows.

Tumors follow a growth curve that slows down as their size increases. Mathematically, this is described by a Gompertzian equation when the tumor is greater than a certain threshold size and by an exponential equation when it is less. In the Gompertzian mode, the volume doubling time of a tumor depends on its size. In the exponential mode, the volume doubling time is equal to the potential doubling time, T_{pot}, and growth is size independent.

In the absence of therapeutic intervention, tumor growth is the result of competing processes of birth and loss of viable cells and is described by the differential equation:

$$\frac{dV}{dt} = (k_b - k_l)V, \qquad \text{Eq. 14}$$

where V is the tumor volume. The birth rate, k_b (= $\ln 2/T_{pot}$), is constant in both exponential and Gompertzian phases. The loss rate, k_l, is 0 in the exponential phase and size dependent in the Gompertzian phase. Explicitly, the size dependence of k_l is expressed by:

$$k_l(V) = 0 \quad \text{and} \quad V < V_G,$$

$$k_l(V) = k_b\left\{\frac{\ln\left(\frac{V}{V_G}\right)}{\ln\left(\frac{V_{max}}{V_G}\right)}\right\}, \quad V \geq V_G, \qquad \text{Eq. 15}$$

where V_G is the Gompertzian transition size (i.e., the size where growth switches from exponential to Gompertzian) and V_{max} is the theoretical upper limit of the Gompertzian growth curve.

Tumor cells sterilized by radiation therapy are not immediately lost from the tumor mass, but become "doomed" and are removed subsequently as time passes. At any time the total tumor volume, V, will consist of the sum of a partial volume, V_v, representing viable tumor cells and another, V_d, representing doomed cells, i.e., $V = V_v + V_d$. The spontaneous loss rate of viable cells is determined by total tumor volume. If the combined rate of loss of viable and doomed cells is greater than the birth rate, the tumor regresses. In the opposite situation, it grows. The number of doomed cells is assumed to decay exponentially with a rate constant, k_s (= $\ln 2/T_s$, where T_s is the shrinkage half- time).

For targeted radionuclide therapy it is assumed that absorbed dose rates will be so low that repair in the tumor cells is complete. This means that tumor cell sterilization is an exponential function of absorbed dose (*18*). No allowance is made in the model for the effects of reoxygenation or redistribution through the cell cycle.

For a tumor irradiated by a low dose rate, r, the rate of change of V_v, is given by:

$$\frac{dV_v}{dt} = (k_b - k_l)V_v - \alpha r V_v, \qquad \text{Eq. 16}$$

where α is the intrinsic radiosensitivity. Note that k_l depends on the total volume and not just the partial volume of viable tumor cells. The rate of change of V_d is given by:

$$\frac{dV_d}{dt} = \alpha r V_v - k_S V_d. \qquad \text{Eq. 17}$$

The rate of change of viable cell number, N, is given by:

$$\frac{dN}{dt} = k_b N - k_l N - \alpha r N. \qquad \text{Eq. 18}$$

This can be reformulated as:

$$\frac{d}{dt}(\ln(S_F)) = (k_b - k_l) - \alpha r, \qquad \text{Eq. 19}$$

where S_F is the surviving fraction (= N/N_0, where N_0 is the initial number of viable tumor cells).

Equations 16, 17, and 19 are solved numerically for V_v, V_d, and S_F, respectively, by Euler's method. From Equations 16 and 17 the

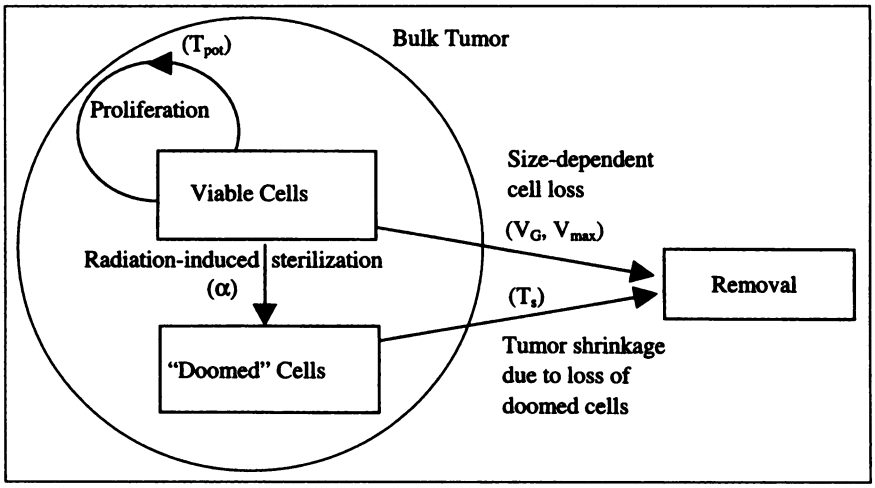

FIGURE 2. Compartmental system describing tumor response. Viable tumor cells are maintained by constant birth rate and tumor size-dependent spontaneous cell loss rate. Exposure to radiation changes status of tumor cells from viable to doomed. Cells are lost from doomed compartment exponentially. Total tumor volume is sum of partial volume associated with viable cells and that associated with doomed cells.

tumor volume during time period i is derived from that at time period i − 1 by:

$$V_{v(i)} = V_{v(i-1)} + ((k_b - k_{l(i-1)})V_{v(i-1)} - \alpha r_{i-1}V_{v(i-1)})\Delta t \quad \text{Eq. 20}$$

and

$$V_{d(i)} = V_{d(i-1)} + (\alpha r_{i-1}V_{v(i-1)} - k_S V_{d(i-1)})\Delta t. \quad \text{Eq. 21}$$

The total tumor volume is:

$$V_i = V_{v(i)} + V_{d(i)}, \quad \text{Eq. 22}$$

and the functional form of $k_l(V)$ is given by Equation 15.

Equation 19 can be approximated by a difference equation and integrated numerically as:

$$(\ln(S_F))_i = (\ln(S_F))_{i-1} + [(k_b - k_{l(i-1)}) - \alpha r_{i-1}]\Delta t. \quad \text{Eq. 23}$$

Normal Tissue Dosimetry

Absorbed doses to the whole body and bone marrow for the treatment schemes considered are calculated for a "standard man" of 70-kg mass with a red marrow mass of 1.5 kg (*19*). The mean absorbed dose to the whole body, D_{WB}, is calculated using MIRD (*20*) methods as:

$$D_{WB} = \tilde{A}_{WB}S_{WB\leftarrow WB}, \quad \text{Eq. 24}$$

where $\tilde{A}_{WB}$, the cumulated activity in the whole body, is given by:

$$\tilde{A}_{WB} = \int_0^\infty (A_{serum}(t) + A_{RB}(t) + A_{tumor}(t))dt, \quad \text{Eq. 25}$$

where the As are the activities in the respective model compartments.

$S_{WB\leftarrow WB}$ is the mean absorbed dose per unit cumulated activity for whole-body–to–whole-body self-irradiation.

Assuming the targeting molecule does not react with blood, bone, or marrow elements, the absorbed dose to red marrow, D_{RM}, is calculated by:

$$D_{RM} = 0.19\tilde{A}_{serum}S_{RM\leftarrow RM} + (\tilde{A}_{WB} - 0.19\tilde{A}_{serum})S_{RM\leftarrow RB}. \quad \text{Eq. 26}$$

The factor 0.19 represents the proportion of the red marrow composed of extracellular fluid with an activity concentration equal to that of serum (*21*).

The S factors (i.e., $S_{WB\leftarrow WB}$, $S_{RM\leftarrow RM}$, and $S_{RM\leftarrow WB}$) were taken from MIRDOSE3 (*22*). $S_{RM\leftarrow RB}$ represents the mean absorbed dose to red marrow per unit cumulated activity in the remainder of the body (excluding red marrow) and was calculated as:

$$S_{RM\leftarrow RB} = S_{RM\leftarrow WB}\left(\frac{mass_{WB}}{mass_{RB}}\right) - S_{RM\leftarrow RM}\left(\frac{mass_{RM}}{mass_{RB}}\right), \quad \text{Eq. 27}$$

where $mass_{RB} = mass_{WB} - mass_{RM}$.

Baseline Model Parameters

The baseline pharmacokinetic parameters are shown in Table 1. The rate parameters (r_1, r_2, and e_1) were taken from an analysis (*17*) of a phase I/II clinical trial of RIT with ^{131}I-labeled murine anti-G250 antibody (*23*). In this study, whole-body and serum activities were examined using a pharmacokinetic model similar to the one used here with the exception that a tumor compartment was not included. When the tumor is small, it has a negligible effect on serum and whole-body pharmacokinetics. These are effectively determined by the values of r_1, r_2, and e_1.

TABLE 1
Baseline Parameter Values for Pharmacokinetic and Radiobiologic Response Model

Parameter	Value
vol_E	3.7 L
τ	2.16×10^{-5}/(h × L)
t_2	0.0295/h
r_1	0.043/h
r_2	0.02/h
e_1	0.024/h
Radiosensitivity (α)	0.35/Gy
T_{pot}	4 d
V_G	0.0056 g
V_{max}	1000 g
T_s	3 d

Tumor activity profiles are governed by the values chosen for the rate parameters τ and t_2. Baseline values of these parameters were derived by assuming that a maximum uptake of 0.025%/g tumor of the injected amount of a trace-labeled quantity of targeting agent occurs at 1.5 d after administration. The values of τ and t_2 that achieve these requirements were derived by iteration and are shown in Table 1.

To enable the calculation of therapeutic response from absorbed dose rate profiles, the following baseline parameter values were used. The intrinsic radiosensitivity (α) of the tumor cells was taken as 0.35/Gy. This represents tumor cells of average radiosensitivity on the scale of experimentally observed in vitro survival curves (*24–26*). The T_{pot} of the tumor cells was taken as 4 d. Again this represents a central estimate of values measured by bromodeoxyuridine labeling in human tumors (*27–30*).

The limiting maximum tumor size (V_{max}) for Gompertzian growth was taken as 1000 g. Together with T_{pot} this sets the value of the Gompertzian transition size (V_G). This is the tumor size at which growth begins to exhibit the continuous slowdown that is characteristic of Gompertzian kinetics. For the given values of T_{pot} and V_{max}, V_G corresponds to 0.0056 g. A value of 3 d was used as an approximate value for the half-time of doomed cell loss (T_s).

An important aspect of the model is that tumor size may vary during treatment. If the growth rate is faster than the rate of cell killing, the tumor size will increase. In contrast, if the rate of cell kill is faster than the growth rate, the tumor shrinks. In either case, the important factor is that the tumor size changes. This means that the absorbed fraction (which is dependent on tumor size) cannot be assigned a single value that is valid over the entire course of treatment. Therefore, in the model simulations, whenever an absorbed dose rate in the tumor was calculated, an absorbed fraction was selected based on the current tumor size. To do this a table of absorbed fractions was consulted at each integration step. The values of absorbed fractions tabulated by Bardiès and Chatal (*31*) were used for this purpose. These were originally calculated based on uniform distributions of radionuclide throughout spheres and represent volume averages.

RESULTS

Treatment Structures

Two treatment structures were examined. The first was an LSA corresponding to the maximally tolerated dose. The second was RF of individually small amounts of radiola-

beled material, each separated by several days. A series of such administrations constituted a course of treatment.

The significant variables for RF therapy are the sizes of the individual administrations and the time gaps between them. In this article a generic RF treatment structure was considered with administrations separated by 3 d. The sizes of individual administrations were set by the requirement that the whole-body burden of radioactivity must not exceed 1.1 GBq (30 mCi) ^{131}I. These values were chosen based on 2 criteria. A high therapeutic intensity is maintained; this precludes excessive time gaps between administrations. The exposure rate at 1 m from the patient is limited to 5 mR/h. For ^{131}I and a "standard man" this restricts whole-body activity to approximately 1.1 GBq.

In the RF schema, dose escalation may be accomplished by increasing the number of fractions in a course until the desired red-marrow or whole-body absorbed dose is achieved.

Two general types of tumor response are considered, cure and remission. On the basis of Poisson statistics, the likelihood of cure is determined by the expectation value of the minimum number of clonogenic tumor cells. For tumors of a given initial size, this is linearly related to the minimum surviving fraction achieved. If a tumor is not cured, it will recur. The remission duration is taken as the time between the start of treatment and tumor regrowth to some size or cell number threshold.

Figure 3 shows the 2 alternative treatment structures. Activity profiles in the whole body are shown for LSA and RF treatments. Both treatment types achieve a red-marrow absorbed dose of 2 Gy and a whole-body absorbed dose of 1.4 Gy. The LSA treatment consists of an administration of 8.25 GBq (223 mCi), whereas RF consists of a total administered activity of 8.61 GBq (233 mCi), given in 11 fractions with 3 d between fractions (i.e., a total treatment time of 30 d). Only the first fraction is 1.1 GBq (30 mCi).

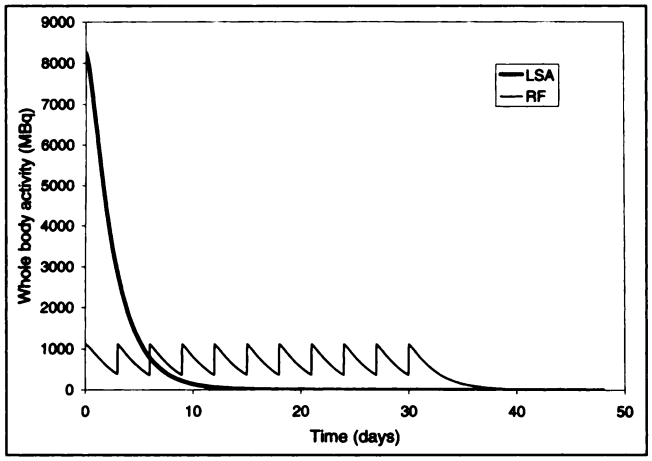

FIGURE 3. Activity profiles in whole body and serum for LSA and RF treatments. Both treatments achieve red-marrow dose of 2 Gy and whole-body dose of 1.4 Gy. LSA treatment consisted of single administration of 8.25 GBq (223 mCi) and RF consisted of total administered activity of 8.61 GBq (233 mCi) delivered in 11 fractions with 3 d between fractions.

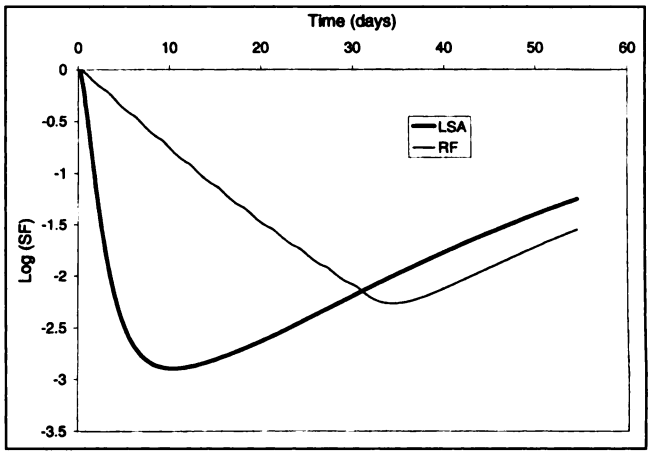

FIGURE 4. Time course of surviving fraction for LSA and RF treatments for macroscopic tumor with initial mass of 100 g. Total absorbed doses in tumor were 20.8 Gy for LSA and 21.3 Gy for RF. For LSA, maximum log cell kill was 2.9, occurring at 10.4 d after administration. For RF, maximum log cell kill was 2.3, occurring at 34.4 d after administration.

Subsequent administrations are smaller because of residual whole-body activity.

Tumor Response

Figure 4 shows the temporal behavior of surviving fraction for a tumor of 100-g initial mass with the baseline response parameters. The total absorbed doses in the tumor were similar (20.8 Gy for LSA; 21.3 Gy for RF). However, the depths of the nadirs of surviving fraction and the times when these occurred were different. For LSA the maximum log cell kill was 2.9 and occurred 10.4 d after administration. For RF this was 2.3, occurring 34.4 d after administration. Peak tumor dose rates were 20.3 cGy/h for LSA but only 3.1 cGy/h for RF.

The time courses of tumor regression and recurrence for the 2 treatments are shown in Figure 5. The rate of regression was faster for LSA than for RF, and the minimum tumor size reached was less for LSA (0.72 g at 27.6 d for LSA versus 1.1 g at 40.0 d for RF). However, tumor regrowth was actually slightly delayed with RF compared with LSA. If remission duration is defined as the time to regrow to a tumor mass of 5 g, then this was 53.2 d for LSA and 61.7 d for RF.

The therapeutic effects for microscopic tumors were also examined. In these simulations the initial tumor mass was set at 1 mg, and all other assumptions and parameters were as previously noted. Figure 6 shows the time course of surviving fraction. Tumor absorbed doses were 12.0 Gy for LSA and 14.9 Gy for RF. Although the RF dose was higher, the nadir of surviving fraction was deeper for the LSA treatment (1.2 logarithms at 6.4 d). The behavior of tumor size is shown in Figure 7. LSA treatment reduced tumor mass to a minimum value of 0.25 mg at 12.8 d after administration. The maximum tumor dose rates achieved were 12.2 cGy/h for LSA and 2.2 cGy/h for RF. In the case of RF, the dose rates were too low to counteract tumor cell

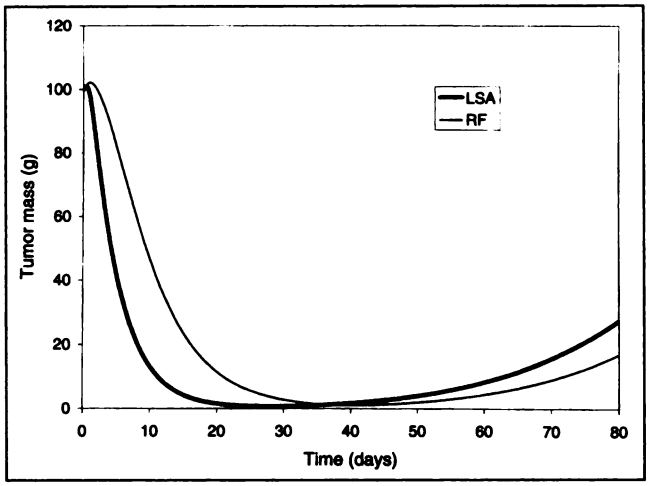

FIGURE 5. Time course of regression and recurrence of macroscopic tumor for LSA and RF treatments. Minimum tumor size reached was 0.72 g at 27.6 d for LSA and 1.1 g at 40.0 d for RF. Tumor regrowth was slightly delayed with RF compared with LSA.

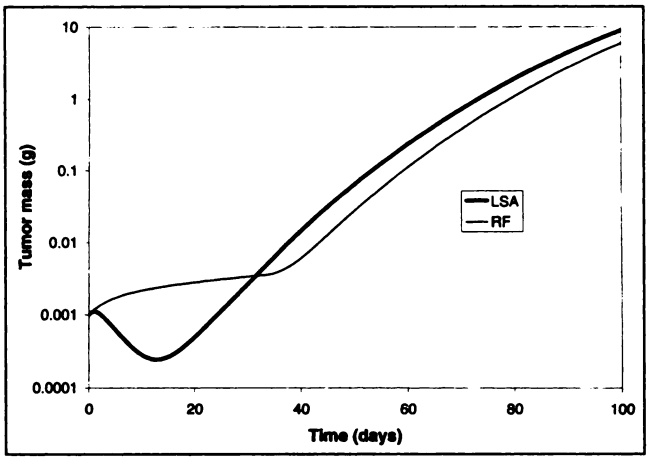

FIGURE 7. Time course of regression and recurrence of microscopic tumor for LSA and RF treatments. LSA treatment reduced tumor mass to minimum value of 0.25 mg at 12.8 d after administration. Although RF treatment failed to reduce tumor size, tumor growth was more delayed than that for LSA.

proliferation, and neither surviving fraction nor tumor size decreased below their initial values. However, in terms of the time for tumors to grow to a given size, RF had a slight advantage. The LSA-treated tumor reached a size of 5 g at 91.9 d, whereas the RF-treated tumor achieved this size at 97.8 d. The full set of responses is shown in Table 2.

It should be noted that the nadirs of surviving fraction and tumor size did not occur at the same time. The nadirs of surviving fraction occurred at 10.4 and 34.4 d after administration for macroscopic tumors treated by LSA and RF, respectively, and at 6.4 d after administration for microscopic tumors treated by LSA. The corresponding nadirs of tumor size occurred at 27.6, 40.0, and 12.8 d after administration. This dissociation is the result of the persistence of the doomed cell volume and indicates that the tumor is actually recurring even as its volume continues to shrink.

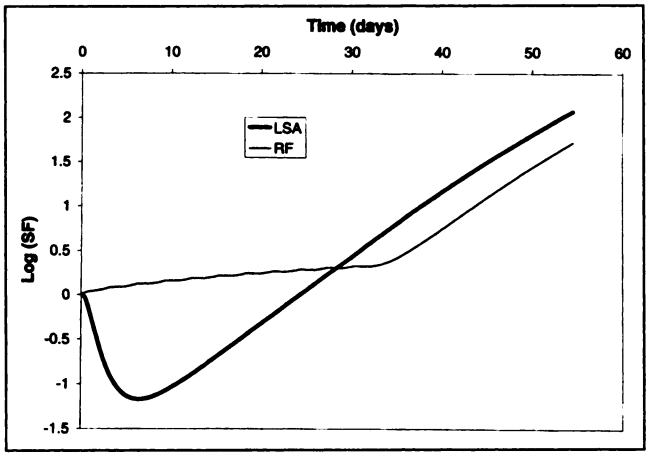

FIGURE 6. Time course of surviving fraction for LSA and RF treatments for microscopic tumor of initial mass of 1 mg. Tumor absorbed doses were 12.0 Gy for LSA and 14.9 Gy for RF. Although RF dose was higher, nadir of surviving fraction was deeper for LSA treatment.

Effects of Changing Model Parameters

The stability of the conclusions of the modeling study was investigated by varying the radiobiologic and pharmacokinetic parameters associated with tumor response.

Table 3 shows the effects on tumor response of varying the radiobiologic parameters over the following ranges: radiosensitivity (α) from 0.2/Gy to 0.5/Gy, T_{pot} from 2 to 7 d, and half-time for doomed cell loss (T_s) from 1 to 7 d. These modifications made little or no differences to the absorbed doses and dose rates in tumors but had varying degrees of impact on response. In all cases cure responses were greater for LSA treatment, whereas remission durations were similar with a slight advantage held by RF treatment.

The relative importance of parameter variation was further examined (Table 4) by calculating the relative changes in response (either nadir of log surviving fraction or time to grow or regrow to 5 g) to LSA therapy caused by a 1% change in the parameters at their baseline values. This was done for both macroscopic and microscopic tumors. Intrinsic radiosensitivity was the most significant determinant of the cure response of tumors of all sizes and remission duration for macroscopic tumors. Proliferation rate was an important determinant of the remission duration of macroscopic tumors and was the most significant factor determining the remission duration of microscopic tumors.

The effect of changing the functional dependency of tumor uptake on size to $t_1(vol_T) = \tau(vol_T)^{2/3}$ was examined. For a spherical tumor, this is equivalent to assuming that tumor uptake is proportional to surface area rather than volume. It has the effect of increasing the relative concentration of activity in smaller tumors. For the purposes of therapy simulation, pharmacokinetic parameters were chosen so that uptake of a trace amount of radiolabel was 0.025

TABLE 2
Calculated Therapeutic Responses for Alternative Treatment Structures for Macroscopic and Microscopic Disease

Tumor size	Treatment	Absorbed dose (Gy)	Peak dose-rate (cGy/h)	Maximum log cell kill	Minimum tumor size	Remission duration (d)
Macroscopic	LSA	20.8	20.3	2.9	0.72 g	52.9
	RF*	21.3	3.1	2.3	1.1 g	61.7
Microscopic	LSA	12.0	12.2	1.2	0.25 mg	91.8
	RF	14.9	2.2	0	1 mg	97.8

Maximum log cell kill = $-\log_{10}$ (nadir of surviving fraction); remission duration = time required for tumors to grow or regrow to 5 g.

percentage injected dose per gram (%ID/g) at 1.5 d after administration in a 1-g tumor.

This change in the nature of tumor uptake had a significant impact on the calculated responses. Macroscopic tumors (100 g) experienced a substantially reduced dose (4.9 Gy for LSA and 5.0 Gy for RF) and the calculated surviving fractions were accordingly greater. Maximum log cell kills were 0.56 for LSA and 0.23 for RF. The duration of remission (defined here as the time required for the tumor to grow back to its original size) was 42.3 and 50.5 d for LSA and RF, respectively. In contrast, responses for microscopic tumors were greatly enhanced. For tumors of initial size 1 mg, the calculated absorbed doses were 129 Gy for LSA and 182 Gy for RF, with calculated maximum log cell kills of 18.5 and 24.6, respectively. It should be noted that the tumor response model breaks down for absorbed doses and radiobiologic effects of this magnitude. Because the calculated cell kills are vastly in excess of those necessary to cure these tumors, the concept of a cell population that goes through a nadir and then regrows is inapplicable.

DISCUSSION

The model used in this article is an integrated description of targeted radionuclide therapy pharmacokinetics and tumor response. The pharmacokinetic model enables the generation of a time–activity profile in the tumor from which absorbed dose rates may be derived. The response model describes the effect these dose rates have on the targeted tumor. To simplify the analysis, it was assumed that absorbed doses and dose rates throughout the tumor are uniform. This is a fundamental assumption.

Two alternative treatment structures were considered, LSA and RF of smaller administrations. In the modeling study, LSA treatment consistently produced a smaller nadir of tumor cell number than did RF. This held for both macroscopic and microscopic tumors and was independent of tumor radiosensitivity, growth kinetics, and uptake characteristics of the targeting agent. However, LSA treatment was not superior to RF treatment in terms of remission duration. Although the differences between the treatment types were small, RF consistently produced longer remission durations or times to recurrence than LSA. Again, this finding was independent of radiosensitivity, kinetics, and the nature of uptake of the targeting agent. It might appear contradictory that LSA is better than RF for one interpretation of tumor response, whereas for another interpretation the opposite holds. This situation arises because cure and remission responses are fundamentally different.

The likelihood of cure is dependent on the nadir of viable tumor cell number and is determined within a time compa-

TABLE 3
Effect of Changing Parameter Values on Tumor Response

	Macroscopic LSA		Macroscopic RF		Microscopic LSA		Microscopic RF	
Response parameter	Cure (log cell kill)	Remission duration (d)	Cure (log cell kill)	Remission duration (d)	Cure (log cell kill)	Remission duration (d)	Cure (log cell kill)	Remission duration (d)
Baseline	2.9	53	2.3	62	1.2	92	0	98
α = 0.2/Gy	1.6	42*	1.1	52*	0.51	82	0	87
α = 0.5/Gy	4.2	77	3.4	84	1.9	102	0.31	103
$T_{1/2}$ = 2 d	2.7	36†	1.6	45†	0.81	47	0	55
$T_{1/2}$ = 7 d	3.0	85	2.6	94	1.4	160	0.4	163
T_s = 1 d	2.8	46	2.1	58	1.1	90	0	97
T_s = 7 d	3.0	63	2.5	70	1.2	93	0	99

*Time to 20 g.
†Time to 10 g.
Cure = $-\log_{10}$ (nadir of surviving fraction); remission duration = time required for tumor to grow or regrow to 5 g, except where otherwise noted.

TABLE 4
Relative Sensitivity of Tumor Response to Changes in Model Parameters

Parameter change	Macroscopic		Microscopic	
	Cure response	Remission duration	Cure response	Remission duration
Radiosensitivity (α)	1.0	1.0	1.0	1.0
T_{pot}	0.07	0.67	0.26	4.0
Doomed cell loss rate (k_s)	0.03	0.15	0.05	0.07

Differences in cure response (nadir of log surviving fraction) or remission duration (time to tumor growth to 5 g) were calculated for 1% change in respective parameters at their baseline values for LSA therapy. Relative sensitivity was defined as ratio of these differences to those caused by changing radiosensitivity (α) parameter.

rable with the duration of treatment. The cure endpoint represents the net effect of competing dynamic processes of cell birth and death. This means that the rate of treatment-induced cell kill is important, and this, in turn, is determined by the absorbed dose rate to the tumor. The cure response will increase if either (or both) of 2 conditions is met: total absorbed dose increases without a decrease in dose rate or dose rate increases without a decrease in total absorbed dose.

If one parameter increases while the other decreases, the cure response could either increase or decrease depending on the details of the changes.

The critical dose rate has been defined (*32–34*) as that value of dose rate at which the rate of radiation-induced cellular sterilization is equal to the growth rate of the tumor cell population. Mathematically this can be expressed as $r_{crit} = \ln 2/(\alpha T_D)$, where T_D is the effective doubling time of the tumor cells. When the tumor dose rate falls to this critical value, the number of viable cells reaches a minimum value. Any absorbed dose that is delivered at a dose rate less than r_{crit} will not reduce the population any further. By their nature, LSA-type treatments deliver the radiation dose to the tumor at a higher dose rate and over a shorter time than RF treatments. The model study shows that the difference in cure response between LSA and RF is greatest for microscopic disease. This is because the population growth rate is faster for microscopic tumors and, in consequence, the critical dose rate is greater. Thus microscopic tumors are especially resistant to treatment at a low dose rate, such as that produced by RF therapy.

Although only one of many possible fractionated treatments was examined in this article, the cure response of an LSA will be greater than any fractionated treatment that is constrained to deliver the same red-marrow or whole-body dose. This is because the tumor dose rate will always be higher for an LSA.

For tumors that are not cured, the remission response describes the effect therapy has on the time to tumor appearance or reappearance after treatment. The time required for a tumor to reach a given size is determined by its growth rate and by the time required for growth to compensate for therapy-induced cell kill. In this case, where response is determined after a period significantly longer than the duration of treatment, the rate of cell killing is irrelevant, only the total amount of cell kill matters. On the basis of the model used here, the total amount of cell kill is simply αD, where α is the radiosensitivity and D is the total absorbed dose. Therefore, remission response depends on the total absorbed dose but does not depend on the dose rate at which this is delivered. The remission response will increase if either (or both) of 2 conditions occurs: total absorbed dose increases without an increase in tumor growth rate or tumor growth rate decreases without a decrease in total absorbed dose.

Just as in the case for cure response, if these parameters change in ways that have opposing effects on remission response, the net effect will depend on how the balance is altered between the total amount of cell kill and the rate of cellular proliferation.

The model study suggests that RF will produce a longer duration of remission than an LSA, although the actual differences are small and arguably negligible. Nevertheless, it is instructive to examine how this result arises for both macroscopic and microscopic disease. For macroscopic tumors, the total absorbed dose to the tumor is similar for both LSA and RF therapy. However, because of its greater rate of cell killing, LSA produces more shrinkage than RF, and this results in a smaller nadir value of tumor size. Because of Gompertzian kinetics, a smaller tumor has a faster growth rate and thus grows to any given size at an earlier time.

For microscopic disease, the growth rate of tumors is exponential and thus size independent. Again, because of its greater rate of cell killing, LSA shrinks the tumor to a smaller size than RF. For tumors in the microscopic range, the absorbed fraction is a rapidly varying function of tumor size. The smaller tumor size produced by LSA has a smaller absorbed fraction and thus experiences a reduced absorbed dose. Therefore, in this case, RF produces a longer duration of remission than LSA, because it delivers a higher absorbed dose to the tumor. For both macroscopic and microscopic tumors, the smaller nadir of tumor size and the better cure response achieved by LSA treatment do not translate into a longer duration of remission.

The sensitivity of the calculated tumor response to the model parameter values was examined. Intrinsic tumor cell radiosensitivity was the main factor determining the depth of the nadir of surviving fraction (cure response), even for rapidly growing microscopic tumors. The remission duration was also dependent on tumor cell radiosensitivity, but proliferation rate was more important than for cure response. For microscopic tumors, the proliferation rate was the most significant determinant of remission duration.

The nature of the uptake characteristics of radiolabeled material has a large impact on the curability of tumors,

especially for microscopic disease. An alternative model in which the concentration of activity increased as the tumor became smaller (i.e., proportional to surface area) yielded calculated log kills that were 10-fold greater than the case in which concentration was assumed to be independent of tumor size (i.e., proportional to volume). This is a significant observation, as experimental data suggest that radionuclide uptake per unit mass is greater in smaller tumors than in macroscopic disease. However, the functional form of this relationship is unknown. It is also significant to note that the model describing tumor response becomes inapplicable when the order of cell kill is similar to that of the initial tumor cell number. This is because it is based on the continuous variables of surviving fraction and tumor size and does not directly address the stochastic nature of tumor cure.

There are several other assumptions built into the model that deserve comment. It is reasonable to assume that the repair of radiation damage in tumor cells will be complete, given the relatively low tumor dose rates encountered in targeted radionuclide therapy. However, no account has been taken of cell-cycle effects. These may possibly lead to radiosensitization caused by radiation-induced blocks in cell-cycle progression (*35,36*) and may favor a more protracted low dose rate treatment such as RF.

It was also assumed that equivalent bone marrow toxicity would be achieved by LSA and RF therapies because red-marrow absorbed doses were equal. However, data from animal models suggest that fractionated therapy may be less toxic (*13–15*), probably as a result of proliferative recovery in bone marrow. This implies that fractionation will enable greater activities to be given than would be possible with an LSA and would thus tend to favor the RF strategy. This possibility was not directly addressed in the model study because, at present, there is no reliable radiobiologic isoeffect model for bone marrow toxicity, although work on this subject is ongoing (*37*).

The limitation on the tumor dose rate produced by RF treatment is largely determined by the allowable whole-body activity. In the current study, this was set to 1.1 GBq (30 mCi) ^{131}I. It is not suggested that this fraction size is optimal. The greater the fraction size (and the shorter the interfraction gap) the higher the average tumor dose rate. Therefore, in terms of cure response, greater activities per administration will be more therapeutically effective than lesser amounts, and closely spaced fractions will be more effective than widely spaced ones. The model studies described in this article reflect a comparison between the therapeutic impact of an LSA and a particular fractionation scheme. However, the general findings will hold for intercomparisons between LSA and any fractionated treatment that is constrained to deliver a similar absorbed dose to whole body or red marrow. In particular, LSA treatment will produce an increased cure response but remission durations will be similar to RF.

The model studies described in this article are dependent on the assumption of uniform dosimetry. However, absorbed dose distributions from targeted radionuclides are characteristically nonuniform. Nonuniform dose distributions are less therapeutically effective than uniform distributions of the same mean absorbed dose (*38*). Moreover, the relative loss in effectiveness is more severe when the mean absorbed dose is larger (*39*). Fractionation may therefore have a therapeutic advantage, if each individual fraction targets (even slightly) different subpopulations of tumor cells. Biologically, this could occur through time-dependent changes in tumor capillary blood flow or treatment-induced perturbations to tumor architecture caused by preceding administrations. A more complete description of the impact of dose nonuniformity in targeted radionuclide therapy is presented elsewhere (*39*).

Taking the results of the study presented here, together with those reported previously (*39*), the most appropriate disease categories for single or multiple fraction treatment may be identified. The optimal disease configuation for an LSA of biologically targeted radionuclides is microscopic disease where growth is rapid and uptake is relatively uniform. The most appropriate role for multifraction administrations is for therapy of slowly growing macroscopic disease, especially if uptake is heterogeneous. Given these contrasting conditions, there is a rationale for combining these approaches in clinical situations in which both disease categories exist simultaneously. Following this argument to its logical conclusion, the LSA should consist of a short-range emitting radionuclide that is better for microscopic disease (*40*), whereas RF therapy should use a longer range emitter that would produce a higher degree of cross-fire in bulky disease with heterogeneous uptake. Ideally this treatment approach would be integrated with a course of conventional treatment (surgery, XRT) to simultaneously treat local disease with occult dissemination.

CONCLUSION

A mathematical model was used to compare different targeted radionuclide therapy protocols. For homogeneous absorbed dose distributions throughout tumors, LSAs are predicted to give a greater likelihood of tumor cure than rapidly fractionated treatments of the same marrow toxicity. The differences between the 2 treatment strategies will be greater for fast-growing micrometastatic disease. Expected remission durations or times to progression are predicted to be similar for both treatment types, with a slight advantage for fractionated treatment. If dose distributions are heterogeneous, RF may have a therapeutic advantage, depending on how tumor uptake varies from one fraction to another. LSAs are better for homogeneous targeting of microscopic disease. RF therapy may be better for heterogeneous targeting of macroscopic disease. There is a rationale for combining both types of therapy in clinical situations in which these disease categories coexist. In this case, the optimal therapeutic strategy may be an LSA using radionuclides with short

emission ranges in combination with fractionated administrations using long-range emitters.

ACKNOWLEDGMENTS

This work was supported in part by National Institutes of Health/National Cancer Institute program project PO1-Ca-33049 and by U.S. Department of Energy grant DE-FG02-86ER60407.

REFERENCES

1. Caron PC, Jurcic JG, Scott AM, et al. A phase 1B trial of humanized monoclonal antibody M195 (anti-CD33) in myeloid leukemia: specific targeting without immunogenicity. *Blood.* 1994;83:1760–1768.
2. Knox S, Hoppe RT, Maloney D, et al. Treatment of cutaneous T-cell lymphoma with chimeric anti-CD4 monoclonal antibody. *Blood.* 1996;87:893–899.
3. Steffens MG, Boerman OC, Oosterwijk-Wakka JC, et al. Targeting of renal cell carcinoma with iodine-131-labeled chimeric monoclonal antibody G250. *J Clin Oncol.* 1997;15:1529–1537.
4. Bentzen SM, Johansen LV, Overgaard J, Thames HD. Clinical radiobiology of squamous cell carcinoma of the oropharynx. *Int J Radiat Oncol Biol Phys.* 1991;20:1197–1206.
5. Fowler JF, Lindstrom MJ. Loss of local control with prolongation in radiotherapy. *Int J Radiat Oncol Biol Phys.* 1992;23:457–467.
6. Petereit DG, Sarkaria JN, Chappell R, et al. The adverse effect of treatment prolongation in cervical carcinoma. *Int J Radiat Oncol Biol Phys.* 1995;32:1301–1307.
7. Withers HR, Taylor JM, Maciejewski B. The hazard of accelerated tumor clonogen repopulation during radiotherapy. *Acta Oncol.* 1988;27:131–146.
8. Trott KR. Cell repopulation and overall treatment time. *Int J Radiat Oncol Biol Phys.* 1990;19:1071–1075.
9. Fowler JF. The phantom of tumor treatment: continually rapid proliferation unmasked. *Radiother Oncol.* 1991;22:156–158.
10. Wheldon TE, O'Donoghue JA. The radiobiology of targeted radiotherapy. *Int J Radiat Biol.* 1990;58:1–21.
11. Dale RG. Dose-rate effects in targeted radiotherapy. *Phys Med Biol.* 1996;41:1871–1884.
12. Vriesendorp HM, Shao Y, Blum JE, Quadri SM, Williams JR. Fractionated intravenous administration of ^{90}Y-labeled B72.3 GYK-DTPA immunoconjugate in beagle dogs. *Nucl Med Biol.* 1993;20:571–578.
13. Schlom J, Molinolo A, Simpson JF, et al. Advantage of dose fractionation in monoclonal antibody-targeted radioimmunotherapy. *J Natl Cancer Inst.* 1990;82:763–771.
14. Buchsbaum D, Khazaeli MB, Liu T, et al. Fractionated radioimmunotherapy of human colon carcinoma xenografts with ^{131}I-labeled monoclonal antibody CC49. *Cancer Res.* 1995;55(suppl):5881s–5887s.
15. Sun LQ, Vogel CA, Mirimanoff RO, et al. Timing effects of combined radioimmunotherapy and radiotherapy on a human solid tumor in nude mice. *Cancer Res.* 1997;57:1312–1319.
16. O'Donoghue JA. The response of tumors with Gompertzian growth kinetics to fractionated radiotherapy. *Int J Radiat Biol.* 1997;72:325–339.
17. Loh A, Sgouros G, O'Donoghue JA, et al. A pharmacokinetic model of ^{131}I-G250 antibody in patients with renal cell carcinoma. *J Nucl Med.* 1998;39:484–489.
18. Steel GG. Cellular sensitivity to low dose-rate irradiation focuses the problem of tumour radioresistance. *Radiother Oncol.* 1991;20:71–83.
19. International Commission on Radiological Protection. *Report of the Task Group on Reference Man.* ICRP publication 23. New York, NY: Pergamon Press; 1975.
20. Loevinger R, Budinger TF, Watson EE. *MIRD Primer for Absorbed Dose Calculations.* New York, NY: The Society of Nuclear Medicine; 1988.
21. Sgouros G. Bone marrow dosimetry for radioimmunotherapy: theoretical considerations. *J Nucl Med.* 1993;34:689–694.
22. Stabin MG. MIRDOSE: personal computer software for internal dose assessment in nuclear medicine. *J Nucl Med.* 1996;37:538–546.
23. Divgi CR, Bander NH, Scott AM, et al. Phase I/III radioimmunotherapy trial with iodine-131 labeled monoclonal antibody (MAb) G250 in metastatic renal cell carcinoma. *Clin Cancer Res.* 1998;4:2729–2739.
24. Steel GG, McMillan TJ, Peacock JH. The radiobiology of human cells and tissues: in vitro radiosensitivity—the picture has changed in the 1980s. *Int J Radiat Biol.* 1989;56:525–537.
25. Weichselbaum RR, Rotmensch J, Ahmed-Swan S, Beckett MA. Radiobiological characterization of 53 human tumor cell lines. *Int J Radiat Biol.* 1989;56:553–560.
26. Fertil B, Malaise EP. Intrinsic radiosensitivity of human cell lines is correlated with radioresponsiveness of human tumors: analysis of 101 published survival curves. *Int J Radiat Oncol Biol Phys.* 1985;11:1699–1707.
27. Terry NH, Meistrich ML, Roubein LD, Lynch PM, Dubrow RA, Rich TA. Cellular kinetics in rectal cancer. *Br J Cancer.* 1995;72:435–441.
28. Tsang RW, Fyles AW, Kirkbride P, et al. Proliferation measurements with flow cytometry Tpot in cancer of the uterine cervix: correlation between two laboratories and preliminary clinical results. *Int J Radiat Oncol Biol Phys.* 1995;32:1319–1329.
29. Bolger BS, Symonds RP, Stanton PD, et al. Prediction of radiotherapy response of cervical carcinoma through measurement of proliferation rate. *Br J Cancer.* 1996;74:1223–1226.
30. Bourhis J, Dendale R, Hill C, et al. Potential doubling time and clinical outcome in head and neck squamous cell carcinoma treated with 70 Gy in 7 weeks. *Int J Radiat Oncol Biol Phys.* 1996;35:471–476.
31. Bardiès M, Chatal JF. Absorbed fractions of 22 potential beta-emitting radionuclides for internal radiotherapy. *Phys Med Biol.* 1994;39:961–981.
32. Dale RG. Radiobiological assessment of permanent implants using tumor repopulation factors in the linear-quadratic model. *Br J Radiol.* 1989;62:241–244.
33. Fowler JF. Radiobiological aspects of low dose rates in radioimmunotherapy. *Int J Radiat Oncol Biol Phys.* 1990;18:1261–1269.
34. O'Donoghue JA. The impact of tumor cell proliferation in radioimmunotherapy. *Cancer.* 1994;73(suppl):974s–980s.
35. Hall EJ, Brenner DJ. The dose-rate effect revisited: radiobological considerations of importance in radiotherapy. *Int J Radiat Oncol Biol Phys.* 1991;21:1403–1414.
36. Williams JR, Zhang YG, Dillehay LE. Sensitization processes in human tumor cells during protracted irradiation: possible exploitation in the clinic. *Int J Radiat Oncol Biol Phys.* 1992;24:699–704.
37. Shen S, DeNardo GL, Jones TD, et al. A preliminary cell kinetics model of thrombocytopenia after radioimmunotherapy. *J Nucl Med.* 1998;39:1223–1229.
38. Humm JL, Cobb LM. Nonuniformity of tumor dose in radioimmunotherapy. *J Nucl Med.* 1990;31:75–83.
39. O'Donoghue JA. The implications of nonuniform tumor doses for radioimmunotherapy. *J Nucl Med.* 1999;40:1337–1341.
40. O'Donoghue JA, Bardiès M, Wheldon TE. Relationships between tumor size and curability for uniformly targeted therapy with β-emitting radionuclides. *J Nucl Med.* 1995;36:1902–1909.